Lowland Technology International date; Volume 22 (2): 304-317
International Association of Lowland Technology (IALT): ISSN 1344-9656

Research Paper

Kinetic, Isotherm and Mechanism in Paraquat Removal by Adsorption Process Using Biochars

N.C. Toan [1], Q.A. Binh [2], D. Tungtakanpoung [3], and P. Kajitvichyanukul [4]

ARTICLE INFORMATION

Article history:

Received: 04 October, 2019
Received in revised form: 20 November, 2019
Accepted: 25 November, 2019
Publish on: 06 September, 2020

Keywords:
Adsorption
Biochar
Paraquat
Kinetic
Mechanism
Pore volume

ABSTRACT

This study aimed to explore the isotherm, kinetic and mechanism of paraquat adsorption in aqueous solution by coconut fiber (CFB), corn cob (CCB), bagasse (BGB) and rice husk (RHB) biochars.The biochar characteristics were identified using SEM, BET, and FTIR. Kinetic and isotherm data were followed the Pseudo-second-order and Langmuir models. The biochars were arranged according to their capacity: CFB (12, 72 mg/g), CCB (10.27 mg/g), RHB (9.72 mg/g), BGB (7.79 mg/g) where specific surface area and pore volume determined the adsorption capacity. The intraparticle diffusion model was used to assess the kinetic rate of the adsorption process, which indicates the rate constant of the external diffusion phase where Kip1 was higher than the Kip2 and Kip3 phases. Film diffusion played a major role in the adsorption process. Pore filling, diffusion, hydrogen bonding, π-π and electrostatic interactions contributed to the mechanism of adsorption. CFB has the highest adsorption capacity (12.72 mg/g), and can be an alternative adsorbent.

1. Introduction

Paraquat (1, 1'-Dimethyl-4, 4'-bipyridinium dichloride in Figure 1) is a herbicide which is widely used to control weeds in agriculture. It is highly soluble in water and is a non-selective compound, and is therefore highly toxic which is why there are many incidents of lung toxicity (Chen and Lua, 2000) and persistent contamination, which can cause serious environmental problems and have adverse effects on humans (Garvilescu, 2005).Therefore, typical treatments for pesticide removal from aqueous solutions are discussed (Foster et al., 1991) and reported by the US EPA in 2011. Conventional environmental treatments include coagulation, softening, sedimentation, filtration, chemical oxidation, carbon adsorption and membrane treatment. Among these treatments, adsorption is one of the most feasible techniques for paraquat removal. Its main advantage over other techniques are low cost, simplicity of use (Wang et al., 2015; Liu et al., 2015) and a variety of alternative adsorbents with high porosity could be used.

Biochar is a promising environmentally friendly (Tan et al., 2015) low-cost (Gwenzi et al., 2017) adsorbent which is carbon-rich and contains abundant functional groups. It can be produced by thermal decomposition processes of biomass sources such as corn cobs, bamboo, pine wood, wood chips or grass, across a pyrolysis temperature range

[1] PhD student at Department of Civil Engineering, Naresuan University, Phitsanulok 65000, THAILAND, hcmtoan@hotmail.com,
[2] PhD student at Department of Civil Engineering, Naresuan University, Phitsanulok 65000, THAILAND, quachanbinh1984@gmail.com,
[3] Department of Civil Engineering, Naresuan University, Phitsanulok 65000, THAILAND, dondej24@gmail.com,
[4] Department of Environmental Engineering, Chiang Mai University, Chiang Mai 50200, THAILAND, kpuangrat@gmail.com
[5]Center of Excellence in Materials Science and Technology, Chiang Mai University, Chiang Mai, 50200, Thailand, kpuangrat@gmail.com
*Corresponding author: kpuangrat@gmail.com
Note: Discussion on this paper is open until March 2021

of 100-700 ^{0}C (Keiluweit et al., 2010; Hao et al., 2013; Kearns et al., 2016), under oxygen-limited conditions. According to a review by Inyang and Dickenson in 2015, adsorption mechanisms in organic contaminants by biochar can include pore filling, diffusion and partitioning, electrostatic interaction, hydrophobic interaction, π-π interaction and hydrogen bonding. Tsai and Chen (2013) used swine-manure-derived biochar synthesized at 400^0 C for 1 hour for the removal of paraquat in an aqueous solution, and its removal may be explained as an ion exchange mechanism. The mechanism by which biochar removes paraquat from the aqueous solution needs to be better understood. Various kinds of biochar made from a variety of substances, such as agricultural waste including coconut fiber, corn cobs, rice husks and bagasse have been studied.

In the present study, the main objective is to explore Paraquat adsorption by different biochars using coconut fiber, corn cobs, rice husks and bagasse biomasses. The specific objectives of this study include: (i) the basic understanding of the characteristics of the different biochars such as surface morphology, surface functional groups, surface charge and surface area; (ii) to determine kinetics and isotherm adsorption; and (iii) to discuss the possible mechanisms of the adsorption process.

2. Materials and methods

2.1 Materials and Synthesis of biochar

The biomass materials were collected from the Faculty of Agriculture, Natural Resources and Environment, Naresuan University, Phitsanulok, Thailand.

The four agricultural wastes are, corncobs, coconut fiber, bagasse and rice husks, which were pyrolysed under the best conditions to obtain biochar. The quantity of the feedstock was 30 (g) and placed in ceramic pots fitted with lids, then they were placed in a furnace (Nabertherm, Germany) at optimum temperatures. Finally, the biochar was milled to produce a suitable particle size and stored at room temperature in sealed glass bottles. Biochar samples were produced from different products such as Bagasse Biochar (BGB) heated to 600^{0}C for 6 h, then washed with HF-H_2SO_4; Coconut Fiber Biochar (CFB) heated to 600 ^{0}C for 4 h, then washed with HCl; Corn Cob Biochar (CCB) heated to 600 ^{0}C for 4 h, then washed with HF; and Rice Husk Biochar (RHB) heated to 500 ^{0}C for 6 h, then washed with HF, and all the chemicals were of analytical grade quality. The biochars were ground and sieved through a 0.5 mm mesh, and to remove excess ash, they were washed with 0.1 M acid, and stirred for 1 h at room temperature, then repeatedly washed with distilled-deionized (DDI) water until the pH reached neutral.

2.2 Material characterization

The surface physical morphology of biochar was examined using a scanning electron microscope (SEM) (Leo 1455VP model, Carl Zeiss Microscopy GmbH, Cambridge, England). Fourier Transform-Infrared spectroscopy (FTIR) was recorded at room temperature on a Perkin Elmer Spectrum BX spectrophotometer, and the infrared spectra was recorded in the 4000-400 cm^{-1} range. The values at the point of zero charge (pHpzc) of the biochar were measured by a Zeta Sizer (Nano ZS 90, Malvern, UK). Moreover, each sample was placed in a 77K liquid nitrogen bath with nitrogen gas adsorbate by Micromeritics TriStar II (Surface Area and Porosity), and the surface area of each sample was calculated by the Brunauer-Emmett-Teller (BET) equation. The pore size distribution over the mesopore region was calculated using the Barrett-Joyner-Halenda (BJH) equation.

2.3 Kinetic and isotherm adsorption experiments

All kinetic and isotherm adsorption experiments were carried out using the batch method. The paraquat solutions were prepared from a stock of 1000 (mg/L) by diluting it in deionized water. The mixture of biochar and paraquat was shaken by an Orbital shaker (MS Major Science) at 120 rpm.

In adsorption isotherm experiments, the variable parameters were diverse with different initial concentrations ranging from 10 to 50 mg/L. The fixed parameters were a solid/liquid ratio of 1.5 g per 1000 mL, and the shaking time of 24h was to obtain equilibrium for a suitable initial pH, for all the experiments.

Basically, the two most well-known adsorption isotherm models are the Langmuir and Freundlich equations, because of their simple application to compare isotherm equations by calculating a correlation coefficient of R^2(Shi et al. 2018). The Langmuir isotherm is the most common model used to quantify the amount of pesticides adsorbed onto biochar as a function of concentration at a given temperature. It considers the adsorption of an ideal pesticide onto an idealized surface of biochar, by the following assumptions:

- First, the surface is homogeneous
- Second, all sites are equivalent
- Third, mono-layer coverage
- Fourth, no interaction between adsorbate molecules

The Langmuir equation is written below (Weber et al. 1972):

$$\frac{C_e}{Q_e} = \frac{1}{bQ_o} + \frac{C_e}{Q_o} \qquad [1]$$

Where Q_e is the weight of the paraquat adsorbed (adsorbent) per unit weight of the adsorbent (mg/g), C_e is the equilibrium concentration of paraquat in solution ((mg/L), Q_o is the maximum adsorption capacity for the monolayer (mg/g) and b is the constant which directly measures the affinity of the adsorption between an adsorbent and an adsorbate (L/mg) (Hamdaoui, O. 2006).

The Freundlich isotherm describes the equilibrium on the heterogeneous surface of the adsorbent. This equation is:

$Q_e = K_F C_e^{1/n}$

Or $\log Q_e = \log K_F + \frac{1}{n} \log C_e$ [2]

Where Q_e is the weight of the adsorbate per unit of weight of the adsorbent (mg/g), C_e is the equilibrium concentration of the adsorbate in solution (mg/L), KF is a constant indicating the adsorption capacity of adsorbent and n is constant (Crini, G et al. 2008).

Q_e in both equations can be calculated by:

$Q_e = \frac{V(C_i - C_e)}{W}$ [3]

Where V is the volume of the solution, C_i is the initial concentration of the adsorbate, C_e is the equilibrium concentration of adsorbate, and W is the weight of the applied adsorbent (Crini, G et al. 2008).

For the kinetic study, the experiments were carried out using 500-mL Erlenmeyer flasks containing 350 mL of paraquat solution at 10-50 mg/L concentration and with a 1.5g/L dosage of biochar. During the experiments, samples were taken at different times from 30 to 1440 min, and the amount of paraquat adsorbed onto the biochar at the time *t* was calculated as follows:

$Q_t = \frac{(C_o - C_t)V}{W}$ [4]

Where C_o (mg/L) is the initial concentration of paraquat and C_t (mg/L) is the residual concentration of paraquat at time *t*, *W* (g) is the mass of used biochar and *V (L)* is the volume of paraquat solution (Liu et al. 2015).

There are three kinetic models: pseudo-first-order, pseudo-second-order and intrapaticle diffusion used to study the basic adsorption process of paraquat onto biochar (Nanseu – Njiki et al. 2010). The pseudo-first-order model was expressed as (Ho and Mc Kay 1998):

$\log (Q_e - Q_t) = \log Q_e - K_1 t$ [5]

The pseudo-second-order model was proposed by Ho and Mc Kay (1998) and used for the study as described in the Equation:

$\frac{t}{Q_t} = \frac{1}{K_2 Q_e} + \frac{1}{Q_e} t$ [6]

The intra-particle model is to plot the amount of paraquat adsorbed versus the square root of time, $t^{0.5}$ as follows (Nanseu – Njiki et al. 2010):

$Q_t = K_{ip} t^{0.5}$ [7]

Where Q_t and Q_e are the amount of pesticide adsorbed per gram of biochar (mg/g) at time *t* and at equilibrium, respectively and K_1 (1/hour), K_2 constant (g/(mg hour) and K_{ip} are sorption rate constants of the pseudo-first-order, pseudo-second-order and intra-particle models, respectively. All the model constants and the correlation coefficient (R^2) were determined.

After the adsorption process, the samples were filtered through GF/C to separate the biochar before using a spectrophotometer. The paraquat concentration was analyzed by a colorimetric method using UV-Vis spectrophotometer (Shimadzu UV-Vis) by reducing paraquat to the blue radical. A sample of the paraquat solution was added with 0.1% sodium dithionite in 0.1 M sodium hydroxide. This mixture was immediately mixed and measured for light absorbance using a spectrophotometer at 600 nm wavelength within 1 minute (AOAC, 2000). All experiments were implemented in duplicate under the same set of conditions.

3. Results and discussion

3.1 Characteristics of different biochars

3.1.1 Surface morphology

The SEM images of biochar are shown as the surface morphology of four types, produced from different biomasses with different porous structures in Figure 2. From this study, it can be seen that the different morphologies have similar characteristics with porous structures. Thus, the porosity of each type of biochar may be a significant factor for the efficient removal of paraquat in the adsorption process. The pores have a variety of different sizes and shapes, such as: (i) coconut fiber biochar refers to CFB in Figure 2(A) from 100 to 270 µm. (ii) corn cob biochar refers to CCB in Figure 2(B) from 80 to 400µm. (iii) rice husk biochar refers to RHB in Figure 2(C) from 60 to 270 µm. (iv) bagasse biochar refers to BGB in Figure 2(D) from 50 to 240 µm. This characteristic can affect the physical adsorption properties of each biochar.

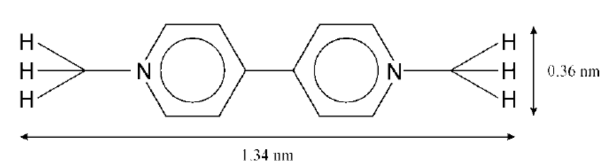

Fig 1. Size of paraquat – an herbicide (Draoui et al. 1999)

3.1.2 Surface charge, surface area of biochar

The solution pH plays a crucial role in the optimization of the adsorption process. Therefore, the pH point of zero charge (pHpzc) in biochar was determined to understand the ability and conditions in which it adsorbs paraquat. Fiol and Villaescusa, (2009) stated that the pH value is the total (net) surface charge of the biochar which has a value of zero, causing it to be neutral. When the pH of a solution is lower than pHpzc, the surface of the biochar is positively charged, and when the pH is greater than pHpzc, it is negatively charged. In this study, the results show that all of the biochars are produced from four types of biomass, which were positively charged when under a very low pH condition (less than between 0.70 and 0.75 in Table 1) and are negatively charged when the pH solution is greater than 1.

The morphologies of the four types produced from different biomasses were presented in Table 1, with pore properties such as Specific Surface Area (SSA), Total Pore Volume (TPV), and pore size distribution. The SSA and TPV of the four types of biochar are enhanced in the order of BGB, RHB, CCB, CFB, respectively, and these pore properties may create good characteristics for pollutant adsorption.

3.1.3 FTIR analysis

The functional groups of the four types of biochar produced from different biomasses, were analyzed using FTIR which clearly displays the peaks indicating the presence of typically functional groups. Specifically, the broad peak near 3789.21 cm^{-1}, 3789.74 cm^{-1} and 3725.38 cm^{-1} , of CFB, CCB and BGB were observed in Fig. 3, and these peaks represented the hydroxyl group (O-H stretching vibration) (Zhang et al. 2011). Some previous studies suggested this group is related to hydrogen-bonding interactions (Zhang et al. 2011 and Chen et al., 2011).

A report by Kinney et al., 2012, sugested that the peaks at 2970.09 cm^{-1}, 2915.56 cm^{-1}, 2916.64 cm^{-1}, 2911.14cm^{-1} of CFB, CCB, RHB and BGB respectively, were refered to as the alkyl group or aliphatic group (C-H stretching vibration) and possessed characteristic of chemical hydrophobicity.

Moreover, the peaks at 2299.83 cm^{-1}, 2383.01 cm^{-1} , 2299.59 cm^{-1} , 2298.66- $cm^{1}$of CFB, CCB, RHB and BGB respectively, were indicated to the ketone group C=O with stretching vibrations (Nuithitikul et al., 2010).
Besides, the possession of bands at 1715.94 cm^{-1}, 1734.47 cm^{-1}, 1716.20 cm^{-1}, 1736.00 $cm^{-1}$of CFB, CCB, RHB and BGB respectively, exhibited for carbonyl groups (C=O) corresponding to various acids, aldehydes, ester and ketones which are mostly formed by dissociation of cellulose and hemicellulose (Liu et al., 2011; Yang et al., 2007 and Liu et al., 2015).

The peaks at 1571.84 cm^{-1}, 1568.03 cm^{-1},1601.57 cm^{-1}, 1563.24 cm^{-1} of CFB, CCB, RHB and BGB respectively displayed the stretching of aromatic C=C (Cheng et al., 2006; Sharma et al., 2004 and Ahmad et al., 2007).

The peaks at 1216.70 cm^{-1},1216.86 cm^{-1},1216.65 cm^{-1} of CFB, CCB, and BGB respectively were related to the aromatic C-O stretching of phenolic hydroxyl (Chun et al., 2004).

On the other hand, the peaks at 1047.05 cm^{-1}, 1045.82 cm^{-1}, 1063.19 cm^{-1}, 1099.12cm^{-1} of CFB, CCB, RHB and BGB respectively, were indicated to the aromatic C-O stretching of alcohol (Saffari et al., 2015). The peaks at 878.86 cm^{-1}, 871.80 cm^{-1}, 791.71 cm^{-1}, 874.50$cm^{-1}$of CFB, CCB, RHB and BGB respectively, indicated the aromatic C-H (Tran et al., 2017).

Table 1 Physical and chemical properties of biochars

Biochar	SSA (m^2/g)	TPV (cm^3/g)	pHpzc	The pore size distributions (%)			
				Micropores (< 2 nm)	**Narrow mesopores (2-20 nm)**	**Mesopores (20-50 nm)**	**Macropores (> 50 nm)**
CFB	402.43	0.151	0.7	17.40	69.22	6.10	7.28
CCB	292.92	0.117	0.75	21.24	56.57	10.39	11.81
RHB	153.27	0.055	0.72	7.90	59.26	13.97	18.87
BGB	67.42	0.029	0.7	16.88	59.29	15.75	8.07

In summary, the FTIR analysis indicated that there are 8 major functional groups on the surfaces of biochar. These can be classified into 2 functional characters, polar groups (hydrophilic characters): Hydroxyl groups (O-H), Ketone groups (C=O), Carbonyl groups (C=O), Aromatic C-O phenolic hydroxyl groups, Aromatic C-O alcohol groups, Aromatic C-H groups and non-polar groups (hydrophobic characters) such as Alkyl groups and Aromatic (C=C) groups. Therefore, the hydrophilic groups account for the main functional groups. This characteristic can indicate that biochar behavior was hydrophilic and agreed with the study by Nanseu-Njiki et al. 2010.

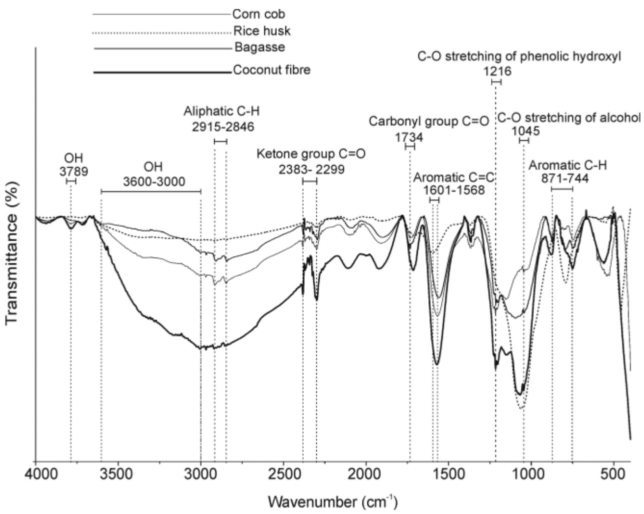

Fig 3. FT-IR spectra analysis of the different biochars

3.2 Effect of pH on Paraquat adsorption onto the biochar

The effect of pH on the efficiency of paraquat removal by four types of biochar was indicated in Fig. 4. In this case, the results showed that all of the biochar produced from different materials had an enhanced percentage of paraquat removal in the pH ranges of 5-7, 9-11, and got the highest PQ removal at pH 11. However, the pH level of the solution in this study was from 1 to 11 and greater than the pH point of zero charge in Table 1, leading to the charge of the biochar being negative.

According to a report by Tantrirantna et al. 2011, the pK_a of cationic paraquat was about 9-9.5. This can explain why, when the pH of the solution is lower than pKa about 9-9.5, the paraquat molecular structure is negatively charged. When the pH of the solution is greater than pKa of paraquat, the molecular structure is positively charged. At pH 11, PQ became positively charged, therefore, PQ can interact efficiently with biochar with a negative charge on the surface based on electrostatic interactions during the adsorption process. This finding is in agreement with the study of Tsai et al. (2003), who similarly noted that the cationic paraquat adsorbed quantitatively onto the negatively charged sites of the adsorbent when the pH values increased due to the loss of H^+ from surface.

3.3 Adsorption Isotherms

Table 2 shows the isotherm parameters of paraquat removal, using four types of biochar produced from different biomasses. There are two common adsorption isotherm models: Langmuir and Freundlich. Because these isotherms can test paraquat adsorption by adsorbents such as activated bleaching earth, activated carbon, clay (Tsai et al. 2003, 2004, 2006; Hamadi et al. 2004). Table 2 illustrated that the adsorption of paraquat on biochar can be described using both Langmuir and Freundlich isotherm models, because both have a suitable correlation coefficient. Considering the values of R^2 of the Langmuir model (0.868 – 0.998) were higher than the values of correlation coefficients of the Freundlich model (0.554 – 0.931), therefore, the adsorption characteristics of paraquat on biochar are obviously described by the Langmuir model.

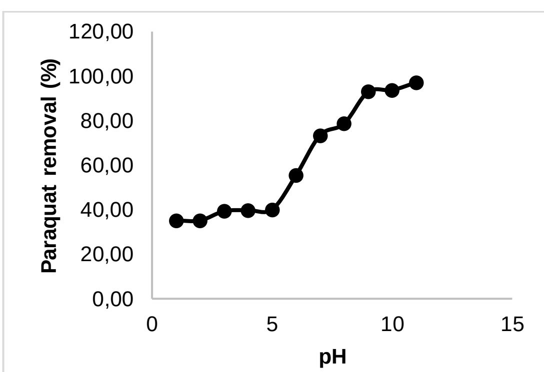

(a) CFB

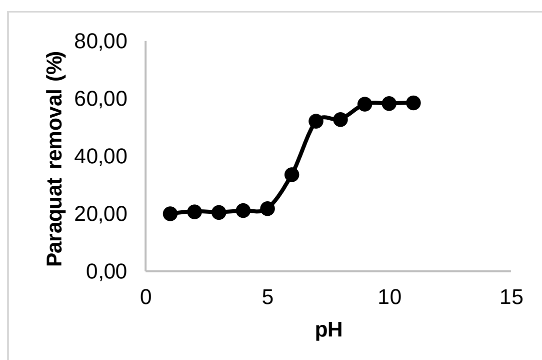

(b) CCB

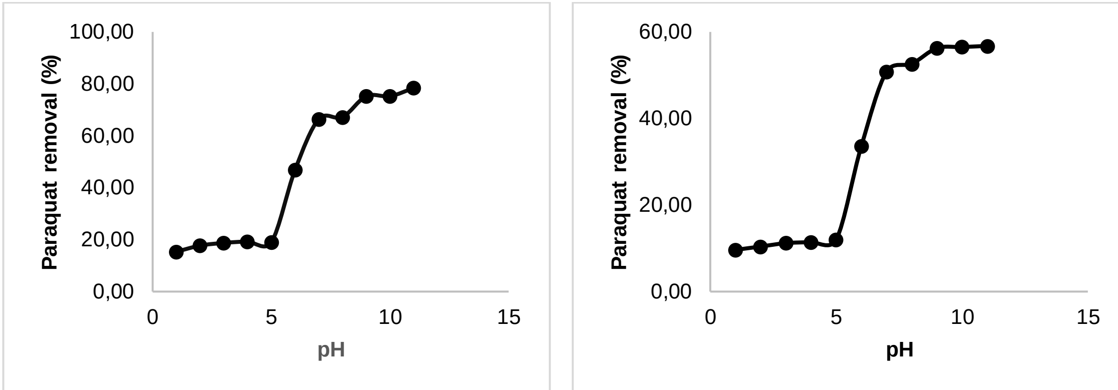

(c) RHB **(d) BGB**

Fig 4. The effect of pH on Paraquat removal by biochars: (a) Coconut fiber, (b) Rice husk, (c) Bagasse, (d) Corn cob (biochar dosage 1 g/L, [PQ] = 3.1 mg/L)

Table 2 Isotherm parameters of paraquat adsorption onto the different biochars

Types of biochar	**Langmuir parameters**				**Freundlich parameters**		
	Qo (mg/g)	**b (L/mg)**	**R^2**	**RL**	**Kf $(mg/g)(L/mg)^{1/n}$**	**1/n**	**R^2**
CFB	12.74	13.08	0.998	$2.31x10^{-3}$	11.39	0.04	0.931
CCB	11.03	0.77	0.868	$3.92x10^{-3}$	6.35	0.18	0.584
RHB	9.90	1.81	0.988	$16.5x10^{-3}$	7.46	0.09	0.554
BGB	7.94	1.24	0.992	$23.78x10^{-3}$	5.11	0.15	0.625

According to a study of Hamdaoui, O.,(2006), the favorable nature of the adsorption process can be defined in terms of the dimensionless separation factor of the equilibrium parameters as follows:

$$\boldsymbol{RL} = \frac{1}{1+bCo} \qquad [8]$$

Where b is the Langmuir constant and Co is the initial concentration of Paraquat in solution. The value of RL indicates the type of isotherm to be irreversible (RL=0), favorable (0<RL<1), linear (RL=1) or unfavorable (RL>1). RL values for paraquat adsorption onto the four types of biochar from $2.31x10^{-3}$ to $23.78x10^{-3}$ were less than 1 and greater than 0, suggesting favorable adsorption. All the above suggests that the Langmuir model fits well for the four types of biochar produced from different biomasses. This means that a monolayer of paraquat can be adsorbed onto the biochars.

3.3 Comparison of paraquat adsorption capacity by the biochars

More interestingly, Figure 5 shows the comparison of the adsorption of paraquat by four types of biochar with different capacities. The following biochars are arranged according to their order of capacity: CFB (12, 74 mg/g), CCB (11.03 mg/g), RHB (9.90 mg/g), BGB (7.94 mg/g), respectively. The coconut fiber biochar has the maximum adsorption capacity that can adsorb 12.74 (mg/g) of paraquat. For this reason, the structure of the four types of biochar in Figure 2 and Table 1 with fundamental pore properties. The first one could be the Specific Surface Area (SSA) of different biochars increased as the consequence in order BGB (67.42 m^2/g) < RHB (153.27 m^2/g) < CCB (292.92 m^2/g) < CFB (402.43 m^2/g). Similarly, the second one can be caused by the Total Pore Volume (TPV) of four types of biochar enhanced in consequence as BGB (0.029 cm^3/g) < RHB (0.055 cm^3/g) < CCB (0.117 cm^3/g) < CFB (0.151 cm^3/g). Therefore, the SSA and TPV can form the nature of the structures of the four types of biochar, and is the reason why their different adsorption capacities of paraquat are CFB (12, 74 mg/g) > CCB (11.03 mg/g) > RHB (9.90 mg/g) > BGB (7.94 mg/g).

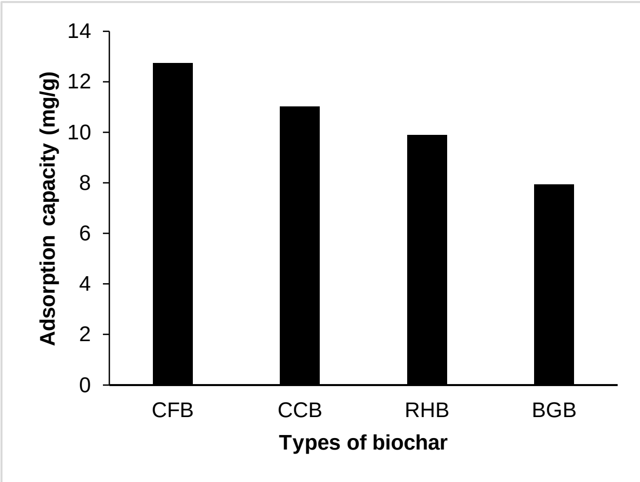

Fig 5. The four types of biochar adsorption capacity of paraquat (Initial paraquat concentrations = 10 - 33 mg/L, adsorbent dosage = 1.5 g/L, Initial pH =11)

Furthermore, the molecular sizes of paraquat are approximately 13.4 A^0 x 3.6 A^0 or 1.34 nm x 0.36 nm in Figure 1 (Draoui et al. 1999). Thus, these pollutants have a smaller molecular size than the pores or pore network of the four types of biochar, therefore, can be easily adsorbed by them. These factors have a strong effect on enhancing the adsorptive capacity of biochar. Hence, this finding can present evidence for the different pore-filling adsorption capacities of biochar by paraquat. A similar study of physical mechanism was conducted by Nguyen et al. (2007) where she indicated that the maximum sorption of contaminants on a natural wood char was reduced when the number of small molecular diameters of aromatic hydrocarbons such as phenanthrene, naphthalene, 1,2-dichlorobenzene, 1,2,4-trichlorobenzene, 1, 4-dichlorobenzene were increased, which was mainly due to the pore-filling mechanism.

3.4 Kinetic adsorption

Figure 6 illustrates the kinetic adsorption of paraquat with an initial concentration of 10 mg/L, 15 mg/l, 27 mg/L by biochars produced from different biomasses. The experiment determined that 4 hours was the time necessary for the adsorption process to reach equilibrium. However, the kinetic studies of Nanseu-Njiki, et. al., (2010) found that it could take only 10 min to complete the adsorption process.

Furthermore, it can be observed that the adsorption process of paraquat occurs more quickly with CCB and BGB which have lower PQ adsorption capacities than the others. This finding is seen in the reaction half time $t^{1/2}$(hour) of CCB and BGB with 0.23 hour around 13.41 – 14.11 minutes in table 3 which was calculated using the following equation Nanseu-Njiki, et. al., (2010):

$$t^{\frac{1}{2}} = \frac{1}{K2qe} \quad (9)$$

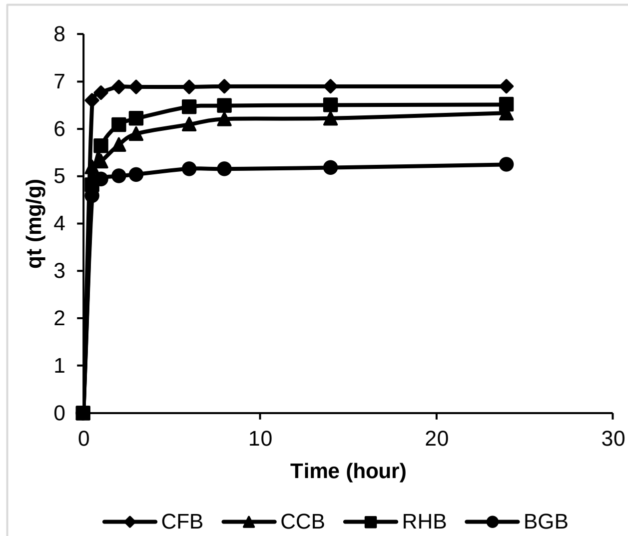

Fig 6. Adsorption kinetics of paraquat onto the biochars (Initial paraquat concentrations: 27 mg/L, adsorbent dosage = 1.5 g/L, and room temperature)

The kinetic parameters of paraquat removal using four types of biochar produced from different biomasses and obtained from the experiments are illustrated in Table 3. The experimental data fitted the Pseudo-first and second order kinetic models. The values of the correlation coefficients (R^2 = 0.9995-0.9998) of the Pseudo-second order model were higher than the values of R^2 (0.683-0.896) of the Pseudo-first order model. Thus, the Pseudo-second order model could adequately describe the kinetic paraquat removal by the adsorption process using the biochars, similar to the kinetic model of adsorption suggested by Tsai et al. 2013 and Kumar et al. 2012.

Moreover, the qe, exp value (12.07 mg/g) is the experimental equilibrium amount of paraquat adsorption onto biochar, agreed very well with the qe, cal (12.15 mg/g) which is calculated from the second-order kinetic model. More importantly, Zhu et al. 2009 studied the pseudo-second order which shows that the kind of adsorption could be chemical. Therefore, this implies that the limiting step of paraquat adsorption on the biochar is by chemisorption.

Table 3 Values of kinetic parameters of paraquat removal by the adsorption process using biochars

Biochar	PQ Conc (mg/L)	Pseudo-first order model				Pseudo-second order model			
		qe exp (mg/g)	Qe,cal (mg/g)	K1 (1/hour)	R^2	Qe, cal (mg/g)	K2 (g/mg hour)	$T^{1/2}$ (hour)	R^2
CFB	27	12.07	4.27	0.19	0.828	12.15	0.23	0.37	0.999
CCB	27	8.60	2.88	0.30	0.896	8.67	0.52	0.23	1.000
RHB	27	9.69	4.09	0.25	0.856	9.82	0.25	0.41	0.999
BGB	27	7.38	2.03	0.23	0.683	7.42	0.58	0.23	1.000

Table 4 Kinetic parameters of paraquat adsorption onto biochar using Intra – particle diffusion model (Initial paraquat concentrations = 27 mg/L, adsorbent dosage = 1.5 g/L, and room temperature)

Biochar	Intra-particle diffusion model								
	Fast adsorption stage			Slow adsorption stage			Equilibrium adsorption stage		
	Cf (mg/g)	Kip1 (mg/g.$h^{1/2}$)	R^2	Cs (mg/g)	Kip2 (mg/g.$h^{1/2}$)	R^2	Ce (mg/g)	Kip3 (mg/g.$h^{1/2}$)	R^2
CFB	0.39	10.41	0.953	9.35	0.55	0.885	8.82	0.82	0.984
CCB	0.14	7.59	0.988	6.43	0.76	0.999	8.03	0.12	0.822
RHB	0.17	7.14	0.981	5.44	1.56	0.959	8.72	0.19	0.983
BGB	0.12	5.72	0.986	6.76	0.11	0.842	6.77	0.13	0.995

According to the study of Tantrirantna et al. 2011, the Intra-particle diffusion model was used to assess the contribution of the diffusion of paraquat in the entire adsorption process. The contribution of this diffusion can be divided into three phases: (1) rapid external diffusion – fast phase refers to paraquat moving easily into macro pores of the biochar (Tantrirantna et al. 2011) with intra-particle diffusion constants (Kip1) of 5.72-10.41mg/g. $h^{1/2}$, (2) slow adsorption phase due to the blocking of micro and meso pores (Liu et al.,2015) with Kip2 of 0.11-1.56 mg/g. $h^{1/2}$, (3) the equilibrium phase with Kip3 of 0.13 – 0.82 mg/g. $h^{1/2}$. Therefore, particle diffusion has a role in the adsorption process. Figure 7 indicates that the linear curve of the Intra-particle diffusion model does not pass through the origin, indicating that the process of paraquat adsorption onto biochar is a complex process (Crini, G et al. 2008). This adsorption process includes both surface adsorption and internal diffusion.

3.5 Mechanisms of the adsorption process

In this study, the biochar adsorption mechanisms for paraquat are discussed below:

3.5.1 Hydrophobic interaction

The properties of paraquat are a polar compound, high solubility in water with 700 g/L (Rodea-Palomares et al. 2015). Paraquat with log Kow = -4.5 at 25^{0}C, this means Kow = $10^{-4.5}$, than 10. Therefore, it can say that paraquat is hydrophilic or soluble (like water) (not a hydrophobic compound due to its low log Kow). Thus, this pollutant is hydrophilic in character. Moreover, the results of FTIR analysis indicated that all biochars possess hydrophilic characteristics. Therefore, the hydrophobic interactions do not contribute to the adsorption mechanisms of biochars for paraquat.

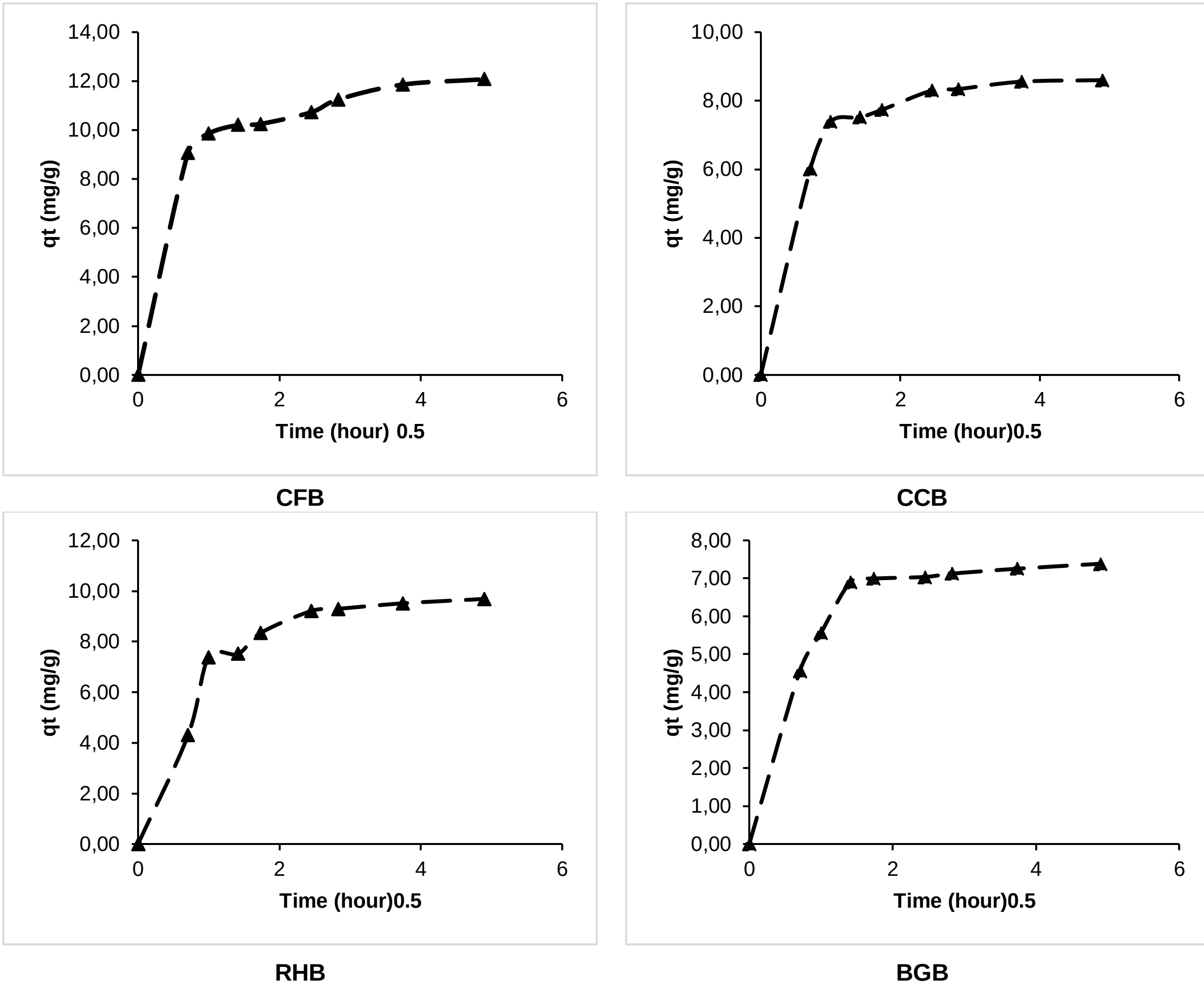

Fig 7. Adsorption kinetics of paraquat onto the biochars using the Intra-particle diffusion model (Initial paraquat concentrations: 27 mg/L, adsorbent dosage = 1.5 g/L, and room temperature)

3.5.2 Pore filling

In this study, the previous results of the values of SSA and TPV in Table 1 and the Paraquat adsorption capacity of biochar have the same sequential consequence CFB >CCB >RHB>BGB, respectively. The molecular size of paraquat are smaller than the pore size of the biochar, thus, these pollutants can fill the pores or the pore network of all four types of biochar. These factors have a strong effect on enhancing the adsorptive capacity of the biochar. Hence, this finding is evidence of enhancing the biochar adsorption capacity for paraquat by increasing the pore sizes of SSA and TPV. A study by Nguyen et al. (2007) indicated that maximum adsorption increased by decreasing the molecular diameter of phenanthrene; naphthalence; 1,2-dichlorobenzene; 1,2,4-trichlorobenzene; 14-dichlorobenzene onto a pitch pine biochar by an adsorptive pore-filling mechanism.

3.5.3 Diffusion

The film diffusion and particle diffusion are two models which can identify the rate-limiting step of paraquat adsorption by the biochars.

The film diffusion model refers to the movement of paraquat onto the external surface of the biochar. The particle diffusion model evaluates the diffusion of paraquat molecules into the pores of the biochar (Nanseu-Njiki et al. 2010 and Liu et al. 2016).

The formula of the particle diffusion model is as follows (Liu et al. 2016):

$$-\ln\left(1-X^2(t)\right) = \frac{D_P\pi^2}{r_o^2}t = k_p t \qquad [10]$$

Where X (t) = q_t/q_e, D_p is the particle diffusion coefficient, r_o is the biochars radius, k_p is used for calculating effective intra-particle diffusivity.

$$k_p = \frac{D_p \pi^2}{r_o^2} \quad [11]$$

The k_p value can be calculated from the slopes of the graph made by plotting –ln (1-X^2 (t)) against t.

The formula of the film diffusion model is as follows:

$$-\ln(1 - X(t)) = k_f . t \quad [12]$$

Where k_f can be calculated from the slopes of the graph that were made by plotting the –ln (1-X(t)) against t, D_f is the film diffusion coefficient.

$$D_f = \frac{k_f r_o \delta C_r}{3C_e} \quad [13]$$

C_e is the concentration of paraquat in the liquid, C_r is the concentration of paraquat as adsorbed by the biochars, δ is the thickness of the liquid film (10^{-5} m) (Liu et al. 2016).

The D_f and D_p values of the film and particle diffusion models for paraquat adsorption into the biochars from the different biomasses are shown in Table 5.

Table 5 Diffusion coefficients and constants for paraquat adsorption onto biochars (Paraquat concentration: 33 mg/L)

Biochar	Parameters of film diffusion model			Parameters of particles diffusion model		
	k_f (h^{-1})	D_f (m^2/s)	R^2	k_p (h^{-1})	D_p (m^2/s)	R^2
CFB	0.240	1.09 x 10^{-11}	0.974	0.229	2.21 x 10^{-13}	0.973
CCB	0.326	1.92 x 10^{-11}	0.923	0.277	4.50 x 10^{-13}	0.977
RHB	0.214	0.87 x 10^{-11}	0.910	0.197	1.51 x 10^{-13}	0.902
BGB	0.304	1.00 x 10^{-11}	0.985	0.286	1.70 x 10^{-13}	0.983
Michelsen et al. 1975		*10^{-10} - 10^{-12} m^2/s*			10^{-15} - 10^{-18} m^2/s	

k_f (h^{-1}): the liquid film diffusion constant, D_f (m^2/s): the film diffusion coefficient

k_p (h^{-1}): the effective intraparticle diffusivity, D_p (m^2/s): the particles diffusion coefficient

By comparing the Dp value of the particle diffusion model in the range of 10-15 - 10-18 m2/s, and the Df value of the film diffusion model in the range of 10-10 - 10-12 m2/s (Michelsen et al. 1975), and the Df values of this study were experienced in the range of 0.87 x 10-11 to 1.92 x 10-11 m2/s, which fitted well to the Df values of Michelsen et al. 1975. On the other hand, the D_p values of the particle diffusion were in the range of 1.51 x 10^{-13} to 4.5 x 10^{-13} m^2/s and were different from the D_p values of Michelsen et al. 1975. Therefore, paraquat adsorption is best described by the film diffusion mechanism, rather than the particle diffusion mechanism. The obvious correlation coefficient was from 0.910 to 0.985. Based on the above kinetic results, it may be noted that the Intra-particle diffusion model is used to describe the adsorption process. These results suggest that the diffusion mechanisms contribute to the adsorption mechanism for paraquat removal.

3.5.4 Electrostatic interaction

The principal of electrostatic interaction is the interaction between a cationic sorbate and an anionic sorbent. It is known that the pKa of cationic paraquat was about 9-9.5 (Tantrirantna et al. 2011 and Rodea-Palomares et al. 2015). Therefore, the paraquat was positivey charged at pH 11. Moreover, the values of the point zero charge (pzc) for biochar were determined as presented in Table 1. The pzc of the biochars were identified in the range 0.70-0.75, lower than 1.0. When the pH solution is greater than pHpzc, the surface of all biochars are negatively charged. Hence, the surface of the biochar is negatively charged at pH 11.

Thus, this indicates that the mechanism of paraquat adsorption onto the biochar closely involves an electrostatic interaction**.**

3.5.5 Hydrogen bonding

Regarding hydrogen bonding formation, the results of the FTIR indicated that the biochars possessed –OH groups, -OH phenolic and alcohol groups, -CH2- groups, carbonyl groups (C=O) corresponding to various acids, aldehydes and ketones,-CH2- groups which formed hydrogen bonding with the hydrogens of paraquat (Figure 8). The hydrogen bonding mechanism is able to occur in 2 cases.

The first case is where the negatively charged oxygen of the functional groups such as –OH, C=O of biochar, interacts with positively charged atoms such as the hydrogens of paraquat (Figure 8A). A similar adsorption mechanism of phenol on biochar was suggested by Liu et al (2011). The study of Liu reported that the enhancement of phenol adsorption by biochar was a major attraction between the oxygen of the functional groups of biochar such as –OH and C=O and phenol molecules based on the hydrogen bond.

In the second case, the attraction between the hydroxyl groups (–OH groups, -OH phenolic groups, -CH2- groups) of biochar and the aromatic rings of paraquat (Figure 8B). This phenomenon is known as Yoshida hydrogen bonding. Blackburn pointed out the interactions between –OH groups of polysaccharide and the aromatic ring residues of dye molecules (Yoshida hydrogen bonding interaction) in 2004. More importantly, Zhu et al. 2009 studied the pseudo-second order model, which shows that the adsorption may be chemical. Therefore, hydrogen bonding plays an important role in the removal of paraquat by biochar.

3.5.6 π-π interaction (π-πelectron donor–acceptor (EDA) interaction)

In considering the π-π interaction between paraquat and biochar, the paraquat molecule has two pyridine rings which possess electron-rich moieties. Thus, these rings can act as π-electron donors to the aromatic rings of biochar. Therefore, it is possible that the π-π interaction between paraquat and biochar can occur (Figure 7C). A study of Hao et al. (2013) suggested that a π-π interaction can happen between the π-electrons of the pesticide as a donor, and the π-electron acceptor in the aromatic rings of the biochar. Hence, the π-π interaction was a relevant adsorption mechanism for paraquat removal by biochar.

3.6 Practical application

Previous studies reported that activated carbon is well known as the prime and oldest adsorbent (Hassler, 1963), but it requires approximately 600 to12000C for the physical activation, and from 4500C to 9000 C for the chemical activation processes using acid or base (Carrot and Carrott, 2007). Furthermore, Ahmad et al., 2014 estimated that the price of activated carbon is approximately US $1476 per ton, while the price of biochar is approximately US $246 per ton. Therefore, the application of biochar can feasibly be applied in developing countries. According to these experimental results, the four types of biochar produced from different biomasses, can be applied and used as alternative economic absorbents, for the removal of pollutant compounds in rural areas.

4. Conclusions

In conclusion, the isotherm data was explained by the Langmuir model. The biochar adsorption capacities for paraquat were determined in reducing order: CFB, CCB, RSB and BGB, based on the surface area and total pore volume. The kinetic data suited the Pseudo-second-order model which is a chemisorption process. The intra-particle diffusion model was used to assess the kinetic rate of paraquat adsorption. Film diffusion has a role in the adsorption process. The adsorption mechanisms could be pore filling, diffusion, hydrogen bonding, π-π and electrostatic interactions. CFB has the highest adsorption capacity (12.72 mg/g), and can be an alternative adsorbent.

Acknowledgement

Authors would like to thank you Thailand Research Fund (Grant No. BRG6180009 and Grant No. IRN62W0005) for the funding support for this work. The authors gratefully acknowledge the support for this study by Naresuan University through the Center of Excellence on Environmental Research and Innovation, Naresuan University and partial support from Center of Excellence in Materials Science and Technology, Chiang Mai University. Moreover, the authors specially thank Mr. Peter Barton and Mr. Kevin Roebl from the Division of International Affairs and Language Development for their editing services of our paper.

References

Admad, M., Rajapaksha, A.U; Lim, J.E., Zhang, M., Bolan, N., Mohan, D., Vithanage, M., Lee, S.S., Ok, Y.S., 2014. Biochar as a sorbent for contaminant management in soil and water: A review. Chemosphere 99, 19-33.

Ahmad, A. L., Loh, M. M., & Aziz, J. A. 2007. Preparation and characterization of activated carbon from oil palm wood and its evaluation on Methylene blue adsorption. Dyes and Pigments, *75*(2), 263-272

Association of Official Agricultural Chemists. 2000. Official methods of analysis of AOAC international, 17th ed., AOAC International, Arlington, VA, USA.

Blackburn, R. 2004. Natural polysaccharides and their interactions with dye molecules: Applications in effluent treatment. Environ. Sci. Technol. 38, 4905-4909.

Carrott, S.P.J.M., Carrott, M.M.L.R., 2007. Lignin-from natural adsorbent to activated carbon: a review. Bioresource Technology, 98, 2301-2312.

Chen, C.M and Lua, A.C. 2000. Lung toxicity of paraquat in the rat. Toxicol. Environ. Health (A) 59, 477.

Chen, C., Lehmann,J., Thies, J.E.., Burton, S.D., Engelhard, M.H. 2006. Oxidation of black carbon by biotic and abiotic processes. Organic Geochemistry. 37, 1477-1488.

Chen, B.L., Zhou, D.Q., Zhu, L.Z., 2008. Transitional adsorption and partition of nonpolar and polar aromatic contaminants by biochars of pine needles with different pyrolytic temperatures. Environmental Science and Technology 42, 5137-5143.

Chen, X., Chen, G., Chen, L., Chen, Y., Lehmann, J., McBride, M. B., & Hay, A. G. 2011. Adsorption of copper and zinc by biochars produced from pyrolysis of hardwood and corn straw in aqueous solution. Bioresource Technology, 102(19), 8877-8884

Chun, Y., Sheng, G., Chiou, C. T., & Xing, B. 2004. Compositions and sorptive properties of crop residue-derived chars. Environmental Science & Technology, 38, 4649-4655.

Crini, G., Gimbert, F., Robert, C., Martel, B., Adam, O., Morin-Crini, N., Griorgi, F. D., Bodot, P. M., 2008. The removal of Basic Blue 3 from aqueous solutions by chitosan-based adsorbent: Batch studies. Journal of Hazardous Materials 153, 96-106.

Coates, J. 2000. Interpretation of Infrared Spectra, A practical Approach. Encyclopedia of Analytical Chemistry, R.A, Meyers (Ed.). Ohn Wiley & Sons Ltd, Chichester. 10815-10837.

Draoui, K., Denoyel, R., Chgoura, M. and Rouquerol, J. (1999). Adsorption of paraquat on minerals. A thermodynamic study. Journal of Thermal Analysis and Calorimetry. Vol. 58, 597-606

Food and Agriculture Organization of the United Nations. 2002. Retrieved 16 April 2011, from International Code of Conduct on the Distribution and Use of Pesticides.

Fiol, N and Villaescusa, I. 2009. Determination of sorbent point zero charge: usefulness in sorption studies. Environmental Chemistry Letters 7 (1): 79-84.

Foster, D. M., Rachwal, A. J., and White, S. L. 1991. New treatment processes for pesticides and chlorinated organics control in drinking water. Water and Environmental Journal, 1, 466-477.

Funke, A., Ziegler, F., 2010. Hydrothermal carbonization of biomass: a summary and discussion of chemical mechanisms for process engineering. Biofuels bioprod. Biorefin. 4, 160-177.

Gavrilescu, M 2005. Fate of pesticides in the environment and its bioremediation. Eng Life Sci 5: 497-526.

Gwenzi, W., Chaukura, N., Noubactep, C., Mukome, F. N.D., 2017. Biochar-based water treatment systems as a potential low-cost and sustainable technology for clean water provision. J. Environ. Manag. 197, 732-749.

Hamadi, N.K., Swaminathan, S and Chen, X.D. 2004. Adsorption of Paraquat dichloride from aqueous solution by activated carbon derived from used tires. Journal of Hazardous Materials B112, 133-141.

Hamdaoui, O. 2006. Batch study of liquid-phase adsorption of methylene blue using cedar sawdust and crushed brick. Journal of Hazardous Material B135, 264-273

Hao, F., Zhao. X,. Ouyang, W., Lin, C,. Chen, S., Shan, Y and Lai, X. 2013. Molecular structure of Corncob-derived Biochars and the Mechanism of Atrazine sorption. Agronomy, Soils & Environmental Quality. Volume 105, Issue 3.

Hassler, J.W., 1963. Activated carbon. Chemical Publishing Company, Inc., New York.

Ho, Y. S., and McKay, G., 1998. A comparison of chemisorption kinetic models applied to pollutant removal on various sorbents. Trans IChemE, Vol 76, Part B, November 1998

Inyang. M and Dickenson. E 2015. The potential role of biochar in the removal of organic and microbial contaminants from potable and reuse water: A review. Chemosphere 134, 232-240.

Kalinke, C., Mangrich, A.S., Marcolino, L.H and Bergamini, M.F. 2016. Biochar prepared from castor oil cake at different temperatures: A voltammetric study applied for Pb^{2+}, Cd^{2+} and Cu^{2+} ions preconcentration. Journal of Hazardous Materials. 318, 526-532.

Kearns, J. P., Wellborn, L. S., Summers, R. S., & Knappe, D. R. U. 2014. 2,4-D adsorption to biochars: Effect of preparation conditions on equilibrium adsorption capacity and comparison with commercial activated carbon literature data. Water Research, 62, 20-28.

Keiluweit, M., Nico, P.S., Johnson, M.G., Kleber, M., 2010. Dynamic molecular structure of plant biomass-derived black carbon (biochar). Environmental Science and Technology 44, 1247 – 1253.

Kinney, T. J., Masiello, C. A., Dugan, B., Hockaday, W. C., Dean, M. R., Zygourakis, K., & Barnes, R. T. 2012. Hydrologic properties of biochars produced at different temperatures. Biomass and Bioenergy, 41, 34-43.

Kumar, R., Jain, S.K., Misra, R.K., Kachchwaha, M., Khatri, P.K. 2012. Aqueous heavy metals removal by adsorption on beta-diketone-functionalized styrene-divinylbenzene copolymeric resin. Int J Environ Sci Technol 9: 79-84.

Liu, N; Charrua, A.B; Weng, C.H; Yuan, X., Ding, F., 2015. Characterization of biochars derived from agriculture wastes and their adsorptive removal of atrazine from aqueous solution: A comparative study. Bioresource Technology 198, 55-62.

Liu, N., Zhu, M., Wang, H., Ma, H., 2016. Adsorption characteristics of Direct Red 23 from aqueous solution by biochar. J. Mol. Liq. 223, 335-342

Michelsen, D. L., Gideon, J. A., Griffith, G. P., Pace, J. E., Kutat, H. L., 1975. Removal of soluble mercury from waste water by complexing techniques. US Dept. Industry, Office of Water Research and Technology. Bull No 74.

Nguyen, T., Cho, H., Poster, D., Ball, W., 2007. Evidence for a pore-filling mechanism in the adsorption of aromatic hydrocarbons to a natural wood char. Environ. Sci.Technol. 41 (4), 1212–1217.

Nuithitikul, K., Srikhun, S., & Hirunpraditkoon, S. 2010. Kinetics and equilibrium adsorption of Basic Green 4 dye on activated carbon derived from durian peel: Effects of pyrolysis and post-treatment conditions. Journal of the Taiwan Institute of Chemical Engineers, 41(5), 591-598.

Rodea-Palomares, I.,Makowski, M., Gonzalo, S., Gonzalez-Pleiter, M., Leganes, F., Fernandez-Pinaz, F. (2015). Effect of PFOA/PFOS pre-exposure on the toxicity of the herbicides 2,4-D, Atrazine, Diuron and Paraquat to a model aquatic photosynthetic microorganism. Chemosphere 139, 65-72.

Saffari, M., Karimian, N., Ronaghi, A., Yasrebi, J., & Ghasemi-Fasaei, R. 2015. Stabilization of nickel in a contaminated calcareous soil amended with low-cost amendments. Journal of Soil Science and Plant Nutrition, 15(4), 896-913

Sharma, R.K., Wooten, J.B., Baliga, V.L., Lin, X., Chan, W.G., Hajaligol, M.R. 2004. Characterization of chars from pyrolysis of lignin. Fuel. 83, 1469-1482.

Shi, W., Guo, F., Wang, H., Liu, C., Fu, Y., and Yuan, S.,2018. Carbon dots decorated magnetic ZnFe2O4 nanoparticles with enhanced adsorption capacity for the removal of dye from aqueous solution. Applied Surface Science 433, 790-797.

Tan, X., Liu Y., Zeng, G., Wang, X., Hu, X., Gu, Y.,0- Yang, Z., 2015. Application of biochar for the removal of pollutants from aqueous solutions. *Chemosphere* 125, 70-85.

Tantriratna, P., Wirojanagud, W., Neramittagpong, S., Wantala, K., and Grisdanurak, N., 2011. Optimization for UV-photocatalytic degradation of paraquat over titanium dioxide supported on rice husk silica using Box-Behnken design. Indian Journal of Chemical Technology, Vol 18, September 2011, pp 363-371.

Tsai, W.T., Lai, C.W. and Hsien, K.J. 2003. The effects of pH and salinity on kinetics of paraquat sorption onto activated clay. Colloids and Surfaces, 224, 99-105.

Tsai, W.T., Lai, C.W. and Hsien, K.J. 2003. Effect of particle size of activated clay on the adsorption of paraquat from aqueous solution. Colloids and Surfaces, 263, 29-34.

Tsai, W.T., Lai, C.W., and Hsien, K.J. 2004. Adsorption kinetics of herbicide paraquat from aqueous solution onto activated bleaching earth. Chemosphere 55, 829 – 837.

Tsai, W.T., Hsien, K.J., Chang, Y.M,. Lo.C.C. 2005. Removal of herbicide paraquat from an aqueous solution by adsorption onto spent and treated diatomaceous earth. Bioresource Technology 96, 657-663.

Tsai, W.T., Lai, C.W. 2006. Adsorption of herbicide paraquat by clay mineral regenerated from spent bleaching earth. Journal of Hazardous Materials B134, 144-148.

Tsai, W.T., Chen, H.R. 2013. Adsorption kinetics of herbicide paraquat in aqueous solution onto a low-cost adsorbent, swine-manure-derived biochar. Int. J. Environ. Sci. Technol. 10: 1349-1356.

Tran, H. N., Wang, Y. F., You, S. J., & Chao, H. P. 2017. Insights into the mechanism of cationic dye adsorption on activated charcoal: The importance of π–π interactions. *Process Safety and Environmental Protection, 107*, 168-180.

(US EPA) US Environmental Protection Agency, 2011. Finalization of Guidance on Incorporation of Water Treatment Effects on Pesticide Removal and Transformations in Drinking Water Exposure Assessments. Office of Pesticide Programs U.S. Environmental Protection Agency, Washington, D.C. 20460.

Vassilev, S.V., Baxter, D., Andersen, L.K., Vassileva, C.G., and Morgan, T.J. 2012. An overview of the organic and inorganic phase compostion of biomass. Fuel 94:1-33.

Weber, J. J., Metcalf, R. L., Pitts, J. N., 1972. Adsorption in physicochemical processes for water quality control. Wiley Interscience, NY, pp. 199-259 (Chapter 5)

Zhang, G., Zhang, Q., Sun, K., Liu, X., Zheng, W. and Zhao, Y. 2011. Sorption of simazine to corn straw biochars prepared at different pyrolytic temperatures. Environment Pollution. 159. 2594-2601.

Zhao, L., Cao, X., Masek, O., Zimmerman, A., 2013. Heterogeneity of biochar properties as a function of feedstock sources and production temperatures. J Hazard Mater 256, 1-9.

Zhou, L., Liu, Y., Liu, S., Yin, Y., Zeng, G., Tan, X., Hu, X., Hu, X., Jiang, L., Ding, Y., Liu, S., Huang, X. 2016. Investigation of the adsorption-reduction mechanisms of hexavalent chromium by ramie biochar of different pyrolytic temperatures. Bioresource Technology 218, 315-359.

Zhu, D., Pignatello, J., 2005. Characterization of aromatic compound sorptive interactions with black carbon (charcoal) assisted by graphite as a model. Environ. Sci. Technol. 39 (7), 2033–2041.

Zhu, D., Kwon, S., Pignatello, J., 2005. Adsorption of single-ring organic compounds to wood charcoals prepared under different thermochemical conditions. Environ. Sci. Technol. 39 (11), 3990–3998.

Zhu, C., Wang, L., Chen, W., 2009. Removal of Cu (II) from aqueous solution by agricultural by-product: peanut hull. Journal of Hazardous Material 168, 739-746.

Xiao, F and Pignatello, J.J (2015). Interactions of triazine herbicides with biochar: Steric and electronic effects. Water Research 80, 179-188.

Yang, H., Yan, R., Chen, H., Lee, D.H and Zheng, C. 2007. Characteristics of hemicellulose, cellulose and lignin pyrolysis. Fuel, 86, 1781-1788.

Yavari, S., Malakahmad, A., Sapari, N.B. (2015). Biochar efficiency in pesticides sorption as a function of production variables – a review. Environ Sci Pollut Res 22: 13824-13841.